

Journal Pre-proofs

Performance analysis of three iteration-free numerical methods for fast and accurate simulation of thermal dynamics in district heating pipeline

Xuejing Zheng, Kaiyu Shi, Yaran Wang, Shijun You, Huan Zhang, Chengzhi Zhu, Liang Li, Shen Wei, Na Wang

PII: S1359-4311(20)33104-5
DOI: <https://doi.org/10.1016/j.applthermaleng.2020.115622>
Reference: ATE 115622

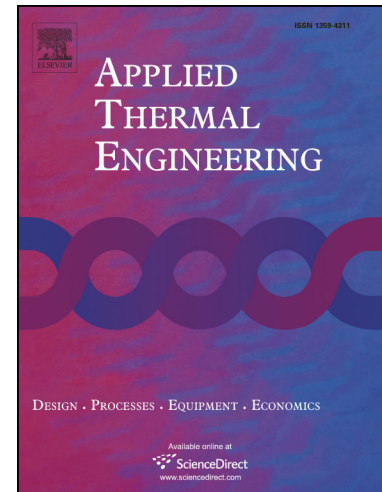
To appear in: *Applied Thermal Engineering*

Received Date: 19 January 2020
Revised Date: 17 May 2020
Accepted Date: 16 June 2020

Please cite this article as: X. Zheng, K. Shi, Y. Wang, S. You, H. Zhang, C. Zhu, L. Li, S. Wei, N. Wang, Performance analysis of three iteration-free numerical methods for fast and accurate simulation of thermal dynamics in district heating pipeline, *Applied Thermal Engineering* (2020), doi: <https://doi.org/10.1016/j.applthermaleng.2020.115622>

This is a PDF file of an article that has undergone enhancements after acceptance, such as the addition of a cover page and metadata, and formatting for readability, but it is not yet the definitive version of record. This version will undergo additional copyediting, typesetting and review before it is published in its final form, but we are providing this version to give early visibility of the article. Please note that, during the production process, errors may be discovered which could affect the content, and all legal disclaimers that apply to the journal pertain.

© 2020 Elsevier Ltd. All rights reserved.



Performance analysis of three iteration-free numerical methods for fast and accurate simulation of thermal dynamics in district heating pipeline

Xuejing Zheng ^{a, b}, Kaiyu Shi ^a, Yaran Wang ^{a, b, *}, Shijun You ^{a, b}, Huan Zhang ^{a, b}, Chengzhi Zhu ^c,
Liang Li ^c, Shen Wei ^d, Na Wang ^a

^a School of Environmental Science and Engineering, Tianjin University, Tianjin 30072, PR China.

^b Tianjin Key Lab of Biomass/Wastes Utilization, Tianjin 300350, PR China.

^c Shijiazhuang Huadian Heating Group Co. Ltd., Shijiazhuang 050041, Hebei Province, PR China

^d The Bartlett School of Construction and Project Management, University College London (UCL), 1-19 Torrington Place, London WC1E 7HB, United Kingdom.

* Corresponding Author: Tel. / Fax: +86 22 2740 0832. E-Mail address: yaran_wang@tju.edu.cn.

Abstract

Numerical methods can provide sufficient information for thermal dynamics of district heating (DH) network. However, high computation burden restricts its application, especially for large-scale DH networks. This dilemma can be overcome by establishing fast numerical calculation procedure and properly selecting the calculation steps without reduction of numerical accuracy. The first-order implicit upwind method is an iteration-free numerical approach for fast simulation of DH pipeline thermal dynamics, while the first-order precision restricts its numerical performance. To further improve the simulation performance, two iteration-free numerical methods with high-order precision, the second-order implicit upwind method and third-order semi-implicit QUICK method are developed. Validations of the three numerical methods are conducted with the measured data of a real DH pipeline. Preferred calculation steps of the three methods are studied via comprehensive numerical experiments. Based on the

preferred step size, simulation comparisons of the numerical methods are performed. Results show that the outlet temperature fluctuations of DH pipeline can be feasibly predicted by these methods with satisfying accuracy. The second-order implicit upwind method perform best considering least computation burden (0.003s) within acceptable error. With the application of the second-order implicit upwind method, simulation analysis on DH pipeline under varying flow velocities are performed.

Keywords: district heating network, thermal dynamics, iteration-free numerical method, efficient numerical simulation, preferred step size

Nomenclature			
T	temperature (°C)	ρ	hot water density (kg/m ³)
U	three-dimensional water velocity (m/s)	λ	thermal conductivity (W/ (m·°C))
c_p	specific heat capacity (J/(kg·°C))	S_T	heat source
u	hot water velocity (m/s)	A	cross section area of the fluid (m ²)
m	mass flow rate of hot water (kg/s)	T_0	soil surface temperature (°C)
R	total thermal resistance (m·°C/W)	h	convective heat transfer coefficient (W/ (m ² ·°C))
d_p	external pipe diameter (mm)	d	internal pipe diameter (mm)
d_i	pipe diameter with insulation (mm)	λ_p	heat conductivity of pipe wall (W/ (m·°C))
λ_i	heat conductivity of insulation (W/ (m·°C))	λ_s	heat conductivity of soil (W/ (m·°C))
z	buried depth (mm)	u^n	hot water velocity at time step n (m/s)
Δx	spatial step (m)	Δt	time step (s)

T_i^n	temperature of control volume i at time step n	T_{in}^n	inlet temperature of DH pipeline at time step n
---------	--	------------	---

1. Introduction

District heating (DH) networks are widely used to deliver heat from heat sources to consumers via heating medium within DH pipelines. Recently, the concepts and technologies on the 4th generation DH (4GDH) have been widely discussed, which represents one of the most important directions of DH techniques. In the 4GDH system, integration of renewables will largely increase the energy efficiency of DH system [1], which requires more flexible network control and effective transient simulation tool of DH networks. Efficient operation and control of DH system are significantly influenced by the thermal dynamic characteristics of DH networks [2], namely the time delay and temperature decay of heating medium transportation. The maximum time delay can be around several hours to more than ten hours for large-scale DH networks [3]. Therefore, studies on thermal dynamic characteristics of DH networks are imperative. Besides, fast and accurate thermal transient calculation method is essential for the efficient thermal dynamic simulation of large-scale DH network [4], as well as the increasing flexibility of DH system.

Steady-state thermal models of DH network have been extensively studied [5, 6]. However, dynamic temperature variation of heating medium within the DH pipeline could not be sufficiently reflected with steady-state thermal models [7]. There are mainly two types of methods for simulating thermal dynamics of DH network: the

statistics-based data-driven modeling methods and modeling methods based on physical mechanism [8]. Statistical model utilizes numerous measured data to achieve model regression of DH system with satisfying accuracy. But such kind of models are deficient in clearly describing the intrinsic physical properties and operation mechanism of DH system, which is important for operation analysis and fault diagnosis. As for physical model, mathematical description is established based on the unsteady heat transfer of DH network, where the temperature variations within each DH pipeline can be efficiently described [9]. Besides, physical model has explicit meaning of parameters and conveys more intrinsic properties of the system.

Earlier study on physical model of DH network was conducted by Kunz et al. [10] with lumped parameter model. In this model, the whole pipe is regarded as a single control volume with linearly distributed temperature. Nevertheless, temperature propagation along the pipeline could not be predicted by this model [11]. Node method is further developed to study the thermal dynamics of DH network [12-16]. Flow time of heating medium in the pipeline is considered as the time delay of DH pipeline. And the variation of the outlet temperature of pipeline is determined by the inlet temperature with time delay and temperature decay. Although node method is simple for simulating thermal dynamics of DH network, there are still some defects when predicting the temperature propagations within DH network [4], and the numerical distortion could generate due to the simplification of physical process [12]. Recently, some new simulation models have been developed, which include plug flow model [17],

trigonometric functions model [9], Modelica based thermo-hydraulic model [18] and thermal-electric analogy transient model [7].

On the other hand, directly solving the partial differential equation (PDE) is another way to efficiently simulate the thermal transients of DH pipeline. Orthogonal collection method was applied to the discretization of PDEs by Biegler et al. [19-21], of which a polynomial was approximate to the differential equation and the equation satisfaction was required at discrete collection points. As for the numerical method, detailed information of DH pipeline thermal transients can be provided with the PDE directly solved [12]. Characteristic line method was proposed and applied to the solution of thermal transient model by Stevanovic et al. [11]. Satisfying agreement between simulated results and measured data was obtained with this model. Zhou et al. [22] also applied characteristic line method to simulate thermal transients of DH system. Lim et al. [23] analyzed the thermal transients of DH system using Simulink based on numerical model. Denarie et al. [24] presented a method for long DH transmission pipeline simulation based on characteristic line method, of which the water thermal capacity could be split between the boundary layer and turbulent core. Besides, Chertov et al. [25] predicted the dynamics of heat front propagating along the pipelines based on the analytical solution. Temperature dynamics was governed by the coupled linear advection-diffusion-heat loss equations, and the equations were solved with general quadrature solution. Among the proposed numerical methods, finite volume methods (FVMs) are widely applied for thermal dynamic analysis. Wang et al. [26] adopted

FVM to discretize the spatial mass conservation equation based on QUICK scheme, and the discrete equation was solved with the utilization of Pressure Implicit Split Operator. Sartor et al. [27] proposed a dynamic model to obtain the temperature and flow rates within DH networks on the basis of one-dimensional FVM. Guelpa et al. [28] proposed a reduced model based on proper orthogonal decomposition coupled with radial basis functions to achieve high-accuracy and fast simulation of DH network. They also analyzed the temperature distribution of DH networks with an upwind scheme [29]. Validation results show that the model was applicable for the dynamic temperature prediction of DH system with good accuracy. Furthermore, a compact physical model was presented to simulate the thermal transients of DH network, which was reliable with mass and energy equation solved [30]. Wang et al. [4] proposed a new third-order numerical method to study the pipeline thermal transient characteristics considering the thermal inertia of pipe wall. Schwarz et al. [31] utilized FVM combined with electric analogy of heat transfer to anticipate the thermal dynamics of DH network. And numerical diffusion of the long DH pipeline was reduced with relatively low computation burden.

FVM is one of the most effective and widely-used numerical methods for solving conservational PDEs. But the applications of numerical methods are restricted by their high computation burden, especially for large-scale DH network. Fast and accurate numerical simulation of DH network thermal dynamics not only relies on effective numerical model and calculation procedure, but also depends on proper selection of

spatial and time steps. Larger time and spatial steps generally enlarge the numerical error, while decreasing the computation burden. Computation performance of the numerical simulation can be improved by using efficient numerical model and appropriately selecting spatial and time steps. However, there are few studies concerning with such topic. Duquette et al. [32] studied the influence of pipe segment length and time step size on computing accuracy and computational intensity of DH pipeline temperature transportation model. Performance of the proposed steady-state variable transport delay model was assessed by the solution of one-dimensional PDE model. But the temperature decay was simply calculated based on steady-state model. Wang et al. [12] performed quantities of numerical experiments to study the optimal spatial and time steps scales of the characteristic line method and their proposed iteration-free first-order implicit upwind method for fast simulation of the DH pipeline thermal transients. The first-order implicit upwind method is an effective approach for solving thermal dynamics of DH pipeline. Calculation speed of this method is very fast, since it can be solved without iteration of linear equations. And due to its implicit numerical scheme, the first-order implicit upwind method can ensure numerical stability without condition. Nevertheless, the first-order implicit upwind method only has first-order precision, which restricts its numerical performance.

Physical modeling methods of DH pipeline thermal dynamics can be generally classified into three categories, the lumped model, the node method and the numerical method. The lumped model was studied by Kunz et al. [10], where the distributed

parameter characteristics cannot be precisely described by this model. For node method, the computation complexities of time and spatial are low, which is suitable for the online operation optimization. But the dynamic transportation of temperature waves along the pipeline fails to be captured with this method and the numerical distortion could generate [12]. As far as numerical method, accurate dynamic predictive information can be provided by this method, while the computation burden is relatively large. This defect can be improved by establishing efficient numerical calculation procedure and properly selecting the calculation steps without reduction of numerical accuracy.

In this paper, two novel iteration-free and high-order numerical methods, the second-order implicit upwind method and the semi-implicit QUICK method, are developed for the calculation of thermal dynamics of DH pipeline. High-efficiency iteration-free calculation procedures are adopted for fast numerical calculation. Validations of the above two methods are performed with measured data of a real DH pipeline located at Shijiazhuang City (China). The preferred spatial and time steps of the two methods and the first-order implicit upwind method are studied via comprehensive numerical experiments. Comparisons of the three numerical methods with their preferred spatial and time steps are performed. With the application of the recommended second-order implicit upwind method, simulation analyses of DH pipeline under varying flow velocities are conducted.

2. Mathematical modeling

Thermal dynamics of hot water within DH pipeline are governed by the law of energy conservation [12, 33]:

$$\frac{\partial(\rho T)}{\partial t} + \nabla \cdot (\rho U T) = \nabla \cdot \left(\frac{\lambda}{c_p} \nabla T \right) + S_T \quad (1)$$

where T denotes the three-dimensional temperature field in pipeline, ρ denotes the density of hot water, U denotes the three-dimensional flow velocity, λ denotes the thermal conductivity and c_p denotes the specific heat capacity of hot water. Besides, the first term of the left-hand side of Eq. (1) represents the unsteady-state term, and the heat convection within the fluid is denoted as the second term of the left-hand side of Eq. (1). For the right-hand side of Eq. (1), the first term represents the conductive heat transfer within the fluid and S_T denotes source term.

Eq. (1) describes the rule of three-dimensional temperature field variation within DH pipeline. For DH networks, the hot water can be regarded as incompressible fluid. Considering only the temperature field along the DH pipe length is focused [12], and taking the heat loss along the pipeline into account, which equals to the source term in Eq. (1), the following one-dimensional PDE pipe model yields [12, 15]:

$$A\rho c_p \frac{\partial T}{\partial t} + mc_p \frac{\partial T}{\partial x} = A\lambda \frac{d^2 T}{d^2 x} + \frac{1}{R}(T_o - T) \quad (2)$$

where A denotes the cross section area of the fluid, m denotes the mass flow rate, T_o denotes the soil surface temperature, and R denotes the total thermal resistance per unit length from the fluid to the ambient environment, which is divided into four parts: convective heat transfer resistance between the hot water and pipe wall, heat conduction

resistance of the pipe wall, insulation layer and the soil [15]. R can be expressed as follow [15]:

$$R = \frac{1}{2\pi h} + \frac{\ln(d_p/d)}{2\pi\lambda_p} + \frac{\ln(d_i/d_p)}{2\pi\lambda_i} + \frac{\ln(2z/d_i)}{2\pi\lambda_s} \quad (3)$$

where h denotes the convective heat transfer coefficient from hot water to the inner wall of the pipe, d_p denotes the external pipe diameter, d denotes the internal pipe diameter, d_i denotes the pipe diameter with insulation, λ_p , λ_i and λ_s denote the heat conductivities of the pipe wall, insulation and soil, respectively, z denotes the buried depth.

In addition, heat conduction along the pipe length is much weaker than that of heat convection [9]. Therefore, the heat conduction term is neglected, and the heat transportation process can be simplified as the following formula [12, 15]:

$$\frac{\partial T}{\partial t} + u \frac{\partial T}{\partial x} = \frac{1}{\rho A c_p R} (T_o - T) \quad (4)$$

where $u = m/(A\rho)$ denotes the hot water velocity. Dynamic temperature distribution along the DH pipeline is described by Eq. (4), which can be solved with initial temperature distribution along the pipeline and inlet temperature of the pipeline.

3. Numerical methods

FVM is one of the most effective and widely-used numerical methods for solving conservational PDEs. The basic idea of FVM is to divide the solution domain into numerous control volumes and assume uniform distribution of the unsolved variables within each control volume. Then the PDE can be approximate to a series of algebraic

equations. Numerical solutions can be therefore obtained by solving these algebraic equations. The accuracy of numerical solution is mainly dependent on the scheme of the algebraic equation and the scales of control volume and calculated time interval.

According to the FVM, DH pipeline can be divided into several control volumes as shown in Fig.1. And the temperature distribution of hot water along the pipeline is assumed uniform for each control volume. For Eq. (4), the time and spatial partial differentials, which correspond to the unsteady-state term and convection term, can be expressed as various finite difference schemes [12, 33].

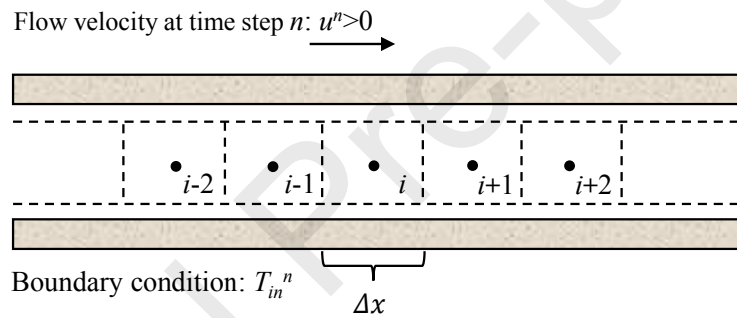


Fig.1. Control volume division of hot water within DH pipeline

3.1. The first-order implicit upwind method

The first-order implicit upwind method can be applied to solve Eq. (4) [12]. Direction of flow rate is considered when determining the hot water velocity within DH pipeline. This method has first-order precision since the temperature on the control surface is influenced by that of the upstream control volume. Time and spatial partial differentials of hot water temperature are replaced by the schemes of implicit difference

and upwind difference, respectively [12, 33]. For $u^n > 0$, the convection term is expressed as:

$$u^n \frac{\partial T}{\partial x} = u^n \frac{T_i^n - T_{i-1}^n}{\Delta x} \quad (5)$$

Eq. (4) can be written as:

$$\frac{T_i^n - T_i^{n-1}}{\Delta t} + u^n \frac{T_i^n - T_{i-1}^n}{\Delta x} = \frac{1}{A\rho c_p R} (T_o - T_i^n) \quad (6)$$

where $n = 1, 2, 3, \dots, N$ and $i = 1, 2, 3, \dots, M$ represent the number of time and spatial steps, respectively, T_i^n denotes the temperature of control volume i at time step n , Δx and Δt denote the sizes of spatial and time steps. Thermal transients of DH pipeline can be solved with boundary and initial conditions: inlet temperature at n th time step (T_{in}^n) and the temperature of each control volume at the previous time step (T_i^{n-1} , $i = 1, 2, 3, \dots, M$).

Eq. (6) can be further rearranged as follow for fast iteration-free calculation [12]:

$$T_i^n = \left(T_i^{n-1} + \frac{\Delta t}{A\rho c_p R} T_o + u^n \frac{\Delta t}{\Delta x} T_{i-1}^n \right) / \left(1 + u^n \frac{\Delta t}{\Delta x} + \frac{\Delta t}{A\rho c_p R} \right), u^n > 0 \quad (7)$$

Temperature of control volume i at time step n can be directly obtained based on Eq. (7). When the flow direction changes ($u^n < 0$), which usually occurs in meshed DH network, the corresponding expression then yields:

$$T_i^n = \left(T_i^{n-1} + \frac{\Delta t}{A\rho c_p R} T_o - u^n \frac{\Delta t}{\Delta x} T_{i+1}^n \right) / \left(1 - u^n \frac{\Delta t}{\Delta x} + \frac{\Delta t}{A\rho c_p R} \right), u^n < 0 \quad (8)$$

The first-order implicit upwind method is unconditionally stable [12], and the calculation procedure of this method is very simple and fast, since in each time step, for calculating the temperature of each control volume, only the temperature at the

previous time step and the temperature of upstream control volume are required, which are already known.

3.2. The second-order implicit upwind method

Similar to the first-order implicit upwind method, flow direction change is also considered for the second-order implicit upwind method. But the temperature on the control surface is determined by that of the two upstream control volumes in this method, therefore, simulation accuracy can be improved to a certain extent compared with the first-order implicit upwind method. For the control volume i , the convection term is expressed as follow, which has second-order precision [33]:

$$u^n \frac{\partial T}{\partial x} = \frac{u_i^n}{2\Delta x} (3T_i^n - 4T_{i-1}^n + T_{i-2}^n) \quad (9)$$

Substitute the unsteady-state term by implicit difference scheme, Eq. (4) is written as:

$$T_i^n = \left(T_i^{n-1} + \frac{\Delta t}{A\rho c_p R} T_o + \frac{\Delta t}{\Delta x} u^n \left(2T_{i-1}^n - \frac{1}{2}T_{i-2}^n \right) \right) / \left(1 + \frac{3\Delta t}{2\Delta x} u^n + \frac{\Delta t}{A\rho c_p R} \right), u^n > 0 \quad (10)$$

For the inverse flow direction, the corresponding expression can also be obtained:

$$T_i^n = \left(T_i^{n-1} + \frac{\Delta t}{A\rho c_p R} T_o - \frac{\Delta t}{\Delta x} u^n \left(2T_{i+1}^n - \frac{1}{2}T_{i+2}^n \right) \right) / \left(1 - \frac{3\Delta t}{2\Delta x} u^n + \frac{\Delta t}{A\rho c_p R} \right), u^n < 0 \quad (11)$$

Two upstream control volumes are considered for the second-order implicit upwind method, which is beneficial to the improvement of simulation accuracy. And the calculation procedure is simple and fast, since the temperature at each control volume can also be directly calculated by solving the algebraic equation Eq. (10) or Eq.

(11) without numerical iteration. Besides, there is no specific condition required for the numerical stability of the second-order implicit upwind method.

3.3. The semi-implicit QUICK method

Another third-order difference scheme for the substitution of convection term in Eq. (4) is QUICK scheme [33]. This difference scheme is introduced for the better comparison of different calculation precision numerical methods, from which the fast and accurate thermal dynamic simulation of DH pipeline can be efficiently obtained.

More information is used to the temperature calculation of each control volume for QUICK method, since the control surface temperature is determined by the temperatures of two upstream control volumes and one downstream control volume.

For $u^n > 0$, the convection term at control volume i can be expressed as [33]:

$$u^n \frac{\partial T}{\partial x} = \frac{u_i^n}{8\Delta x} (3T_{i+1}^n + 3T_i^n - 7T_{i-1}^n + T_{i-2}^n) \quad (12)$$

Substitute the unsteady-state term by implicit difference scheme, Eq. (4) can be further written as:

$$\left(1 + \frac{3\Delta t}{8\Delta x} u^n + \frac{\Delta t}{A\rho c_p R}\right) T_i^n = T_i^{n-1} + \frac{\Delta t}{A\rho c_p R} T_o + \frac{\Delta t}{\Delta x} u^n \left(-\frac{1}{8} T_{i-2}^n + \frac{7}{8} T_{i-1}^n - \frac{3}{8} T_{i+1}^n\right), u^n > 0 \quad (13)$$

In order to accelerate the numerical calculation process, temperature of control volume ($i+1$) at n th time step is replaced by the temperature at ($n-1$)th time step, which yields a iteration-free semi-implicit QUICK method. Eq. (13) can be written as follow:

$$T_i^n = \left(T_i^{n-1} - \frac{3\Delta t}{8\Delta x} u^n T_{i+1}^{n-1} + \frac{\Delta t}{A\rho c_p R} T_o + \frac{\Delta t}{\Delta x} u^n \left(\frac{7}{8} T_{i-1}^{n-1} - \frac{1}{8} T_{i-2}^{n-1} \right) \right) / \left(1 + \frac{3\Delta t}{8\Delta x} u^n + \frac{\Delta t}{A\rho c_p R} \right), u^n > 0 \quad (14)$$

Similarly, for the inverse velocity ($u^n < 0$), corresponding expression can be derived:

$$T_i^n = \left(T_i^{n-1} + \frac{3\Delta t}{8\Delta x} u^n T_{i-1}^{n-1} + \frac{\Delta t}{A\rho c_p R} T_o - \frac{\Delta t}{\Delta x} u^n \left(\frac{7}{8} T_{i+1}^n - \frac{1}{8} T_{i+2}^n \right) \right) / \left(1 - \frac{3\Delta t}{8\Delta x} u^n + \frac{\Delta t}{A\rho c_p R} \right), u^n < 0 \quad (15)$$

This method is a kind of explicit scheme with third-order precision. For numerical stability, the Courant-Friedrichs-Lewy (CFL) condition must be satisfied [11, 12, 34], which is expressed as:

$$\Delta x / \Delta t > u^n \quad (16)$$

Eq. (16) shows that the scales of spatial and time steps for the semi-implicit QUICK method are restricted.

4. Results and discussion

Simulation codes of the three FVMs are realized in MATLAB environment. Model validation is performed with the measured data of a real DH pipeline in Shijiazhuang City (China). And numerical experiments are conducted for the selection of preferred spatial and time steps of each numerical method. Comparisons of the three numerical methods with their preferred spatial and time steps are performed for fast and accurate thermal transient prediction of DH pipeline. And thermal transient analyses on DH pipeline under varying flow velocities are performed with the application of the second-order implicit upwind method.

4.1. Validation of the proposed methods

The measured data is from Ref. [12], and topological structure of the DH pipeline is shown in Fig. 2. Hot water is delivered from Luhua combined heat and power plant to heating substation with the total length up to 9.25 kilometers. Inner diameter of the

pipeline is 1400mm. Measurements were conducted on Dec 15th, 2015, where heat source temperature was obtained with three-minute interval measurement at heat source, and the hot water temperature and mass flow rates were obtained with five-minute interval measurement at heating substation. The maximum measurement errors of temperature sensor and electromagnetic flowmeter are 0.4°C and $0.01\text{m}^3/\text{h}$. Linear interpolation is adopted to obtain more values between sampling time instances. Besides, the soil surface temperature T_0 and ambient temperature are assumed to be equal [32], and the average ambient temperature is -10°C during recording. For validating the three numerical methods, the value of R is determined by the regression method between the numerical model and measured data, which is realized in MATLAB Optimization Toolbox with a least square problem solved [12]. And the value of R is $0.35\text{m}\cdot^{\circ}\text{C}/\text{W}$ in this case. Fig.3 shows the measured temperatures at inlet and outlet of DH pipeline. As is shown, the temperature decay at the peak of temperature wave is 0.7°C . And the time delay can be up to 1.5 hours. Besides, the initial temperature distribution along the pipeline are assumed to be constant (88.5°C in this case), which equals to the first term of inlet temperature vector. And the validation tests are conducted based on the successively updated temperature distribution. Fig.4 shows the hot water velocity, which varies between 1.62 m/s and 1.76 m/s .

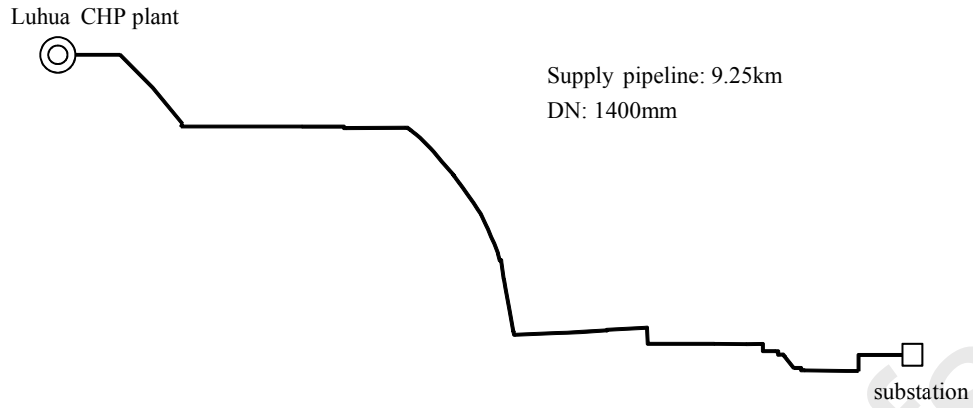


Fig.2. Structure of the measured pipeline [12]

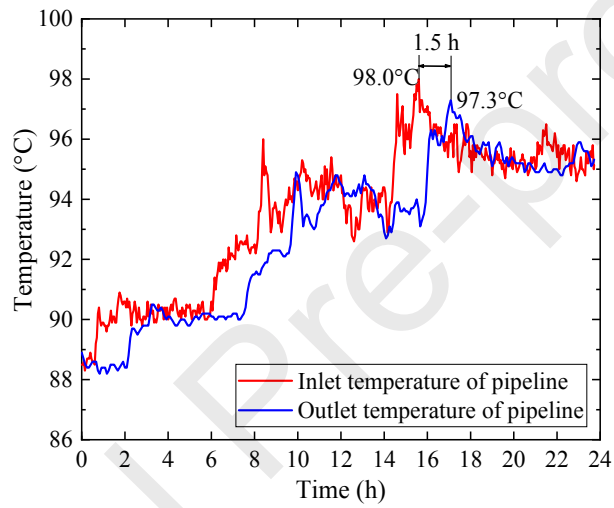


Fig.3. Inlet and outlet temperatures of DH pipeline [12]

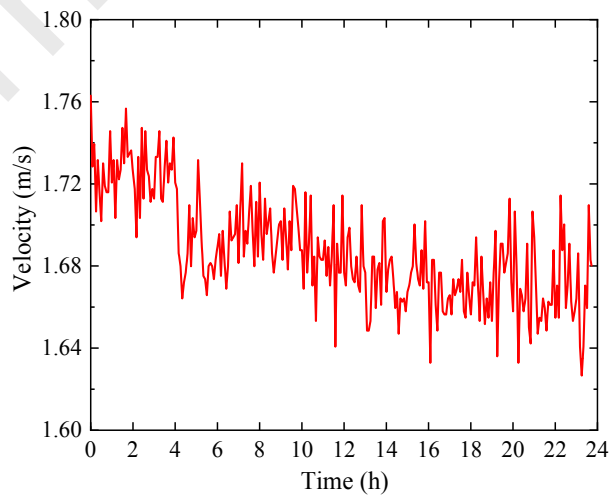


Fig.4. Hot water velocity within DH pipeline [12]

Outlet temperature prediction of DH pipeline with three numerical methods are shown in Fig.5 with the spatial and time steps selected as $\Delta t = 30$ s and $\Delta x = 180$ m. The calculations were conducted on a computer with four-core, 2 GHz CPU and 8 GB RAM. And computation times were recorded using the MATLAB commands “tic & toc”. Fig. 5 shows that the temperature fluctuations of outlet pipeline can be predicted by the three numerical methods with same spatial and time steps, but the calculation errors (difference between calculated value and measured value) of the three methods are different as shown in Fig. 6. And the maximum calculation error for the semi-implicit QUICK method is around 2.0°C. Besides, computation cost is also different for the three numerical methods under same calculation steps. Considering the numerical performance is concerned with the scales of control volume and computing interval, the spatial and time steps are required to be appropriately selected for fast and accurate thermal dynamic simulation.

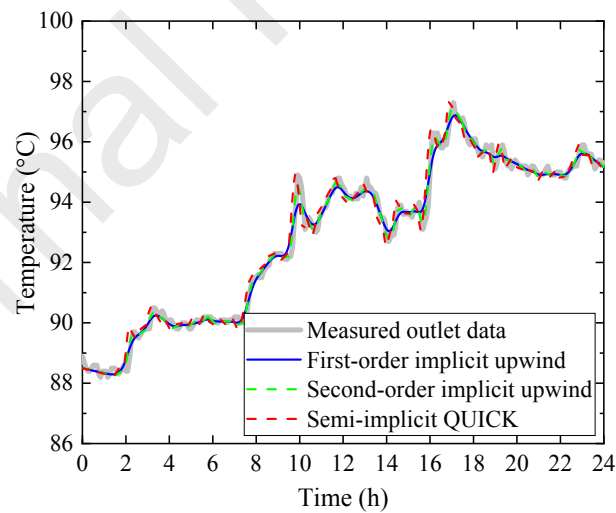


Fig.5. Outlet temperature prediction of the three methods ($\Delta t = 30$ s and $\Delta x = 180$ m)

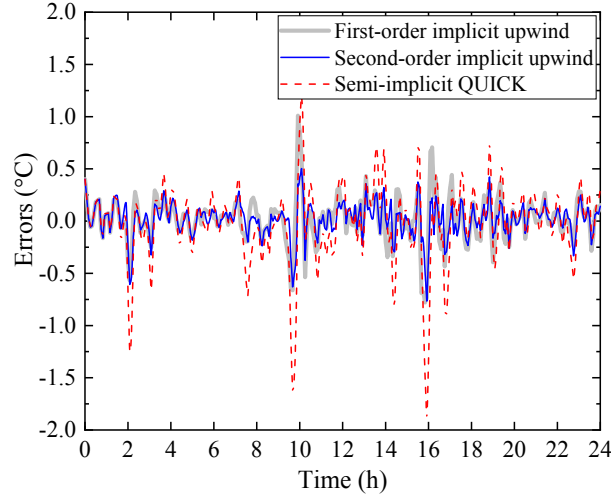


Fig. 6. Calculation errors of the three methods ($\Delta t = 30$ s and $\Delta x = 180$ m)

4.2. Preferred spatial and time steps of the three numerical methods

Comprehensive simulations are performed to obtain numerous results under different sizes of spatial and time steps. For the semi-implicit QUICK method, calculation steps are selected in the cases that the CFL condition is satisfied. Computation burden and calculation accuracy are adopted to measure the simulation performance of the three numerical methods. And the maximum calculation error (denoted as simulation error) is restricted within $\pm 1.0^\circ\text{C}$ considering that the prediction error of 1.0°C in DH system is tolerable in most cases. The preferred spatial and time steps are obtained with the least computation burden, while ensuring simulation errors within $\pm 1.0^\circ\text{C}$.

The computation times and simulation errors of the three numerical methods are shown in Fig. 7. It is shown that with the spatial step increasing, simulation errors of the three methods behave completely different. And the simulation errors of the first-order implicit upwind method monotonously increase as sizes of spatial step increase, while for the second-order implicit upwind method, simulation errors tend to be consistent at the first stage and then increase as spatial step size increases. And the

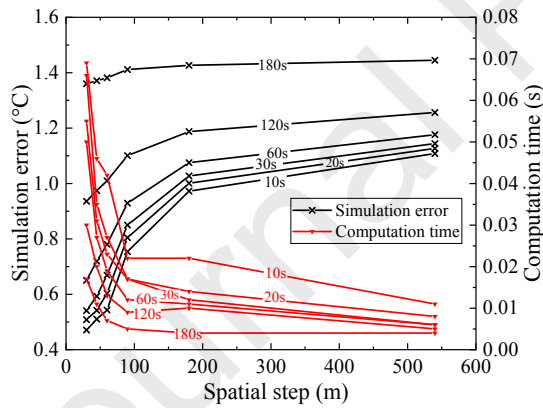
transition point (the point connects the first stage and the second stage) is $\Delta x/\Delta t = u^n$ under each time step. Besides, the first stages embody larger scales of spatial step when the sizes of time step get larger. Meanwhile, for the semi-implicit QUICK method, simulation errors decrease at first and then increase, which can be attributed to the explicit characteristic of the semi-implicit QUICK method and the calculation accuracy could be influenced by the CFL condition, and the least simulation error can be obtained when the pipeline is divided into nine control volumes. In addition, for the three numerical methods, computation burdens decrease as the size of spatial step increases since the pipeline is divided into less control volumes for the larger spatial step. And Fig. 7 also shows that the computation times are relatively small under different spatial and time steps, since the thermal transients of DH pipeline can be simply simulated without iteration. But the difference of computation burden exists, which can be highly enlarged for the thermal dynamic analysis and operation optimization of large-scale DH network with thousands of pipelines.

To ensure acceptable simulation error while reducing the computation burden, the spatial steps should be restricted at $90\text{m} \leq \Delta x < 180\text{m}$ for the first-order implicit upwind method, since the computation burdens are larger for the smaller spatial steps and the simulation accuracy cannot be satisfied for larger spatial steps. Besides, the time steps are required to be within 120s, otherwise the fast inlet temperature variation of DH pipeline could not be captured under larger time step sizes. For obtaining the least computation burden, the spatial and time steps are selected as $\Delta x = 90\text{ m}$ and $\Delta t = 60\text{ s}$, respectively, and the computation time is around 0.012s.

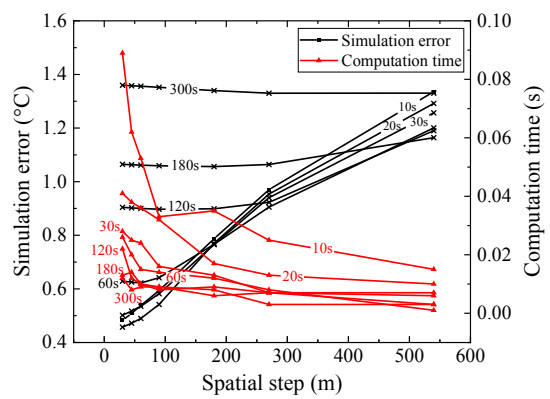
For the second-order implicit upwind method, larger calculation steps ($\Delta x > 270\text{ m}$ and $\Delta t \geq 180\text{ s}$) can lead to unsatisfactory simulation accuracy, since the more detailed changes of pipeline inlet temperature and the more specific information of pipeline are

neglected under these conditions. Moreover, computation times will be highly enlarged under small sizes of calculation steps ($\Delta t < 30$ s and $\Delta x < 90$ m). Considering the acceptable simulation error, the spatial and time steps are recommended as $90\text{m} \leq \Delta x \leq 270\text{m}$ and $30\text{s} \leq \Delta t \leq 120\text{s}$. And the least computation time is 0.003s in the case of $\Delta t = 120$ s and $\Delta x = 270$ m, which is much smaller compared with the first-order implicit upwind method.

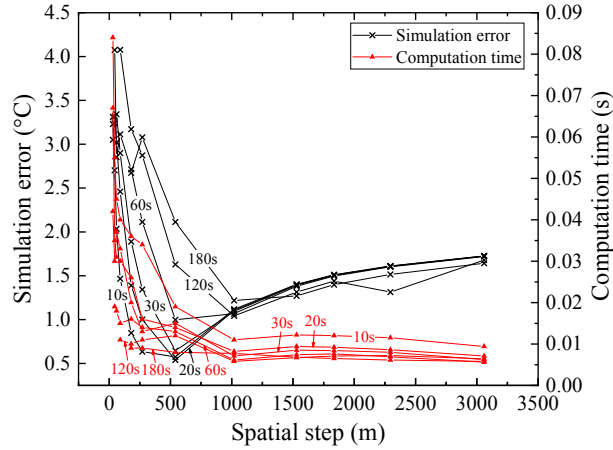
As far as the semi-implicit QUICK method, the unsatisfactory simulation accuracy is observed in the cases $\Delta x > 540\text{m}$ or $\Delta t > 60\text{s}$. And the computation burden approaches constant when $\Delta x > 540\text{m}$, which means that the calculation speed could not be accelerated by enlarging the spatial and time step sizes. Taking both the simulation accuracy and computation burden into account, the sizes of spatial and time steps are selected as $\Delta x = 540$ m and $\Delta t = 60$ s, and the computation time is 0.013s.



(a) The first-order implicit upwind method



(b) The second-order implicit upwind method



(c) The semi-implicit QUICK method

Fig.7. Simulation errors and computation times for the three methods

4.3. Comparison of the three methods with their preferred steps

The recommended spatial and time steps of the above three numerical methods are summarized in Table 1. It shows that the recommended spatial and time steps are different for the three methods. And the higher precision of the method, the larger spatial step is recommended. As for recommended time steps, the time step of the second-order implicit upwind method is larger than that of the semi-implicit QUICK method, which can be attributed to the influence of CFL condition on the latter and the scales of calculation steps and the simulation accuracy are restricted. Computation times of the three methods with the recommended spatial and time steps are also concluded in Table 1, of which the second-order implicit upwind method performs best in computation burden reduction compared with other two methods. And the computation speed of the former is four times than the other two methods. Meanwhile, it should be noted that the calculation uncertainty of the software exists, and the results

of computation time for the three numerical methods indicate there is an order of magnitude difference of the computation cost between the second-order implicit upwind method and the other two methods, which is of great significance to the thermal transient prediction and operation optimization of large-scale DH networks.

Table 1 Simulation results for the three methods

Difference schemes	Time step (s)	Spatial step (m)	Computation time (s)
First-order implicit upwind	60	90	0.012
Second-order implicit upwind	120	270	0.003
Semi-implicit QUICK	60	540	0.013

Fig. 8 shows the outlet temperature prediction of DH pipeline with the three methods utilizing their recommended spatial and time steps. As is shown that the thermal dynamics are well captured with the three methods. Calculation errors of the three methods are shown in Fig. 9. It indicates that with their appropriate spatial and time steps, calculation errors can be ensured within $\pm 1.0^{\circ}\text{C}$. The semi-implicit QUICK method performs best at temperature wave peaks, but the calculation errors are relatively high when the simulation temperature is lower than that of the measured (in the cases that the calculation errors are negative). And numerical instability of the semi-implicit QUICK method can occur under high or abrupt changed flow velocity, while

other two implicit upwind methods are unconditionally stable and the simulation difference between the two implicit upwind methods is relatively small (within 0.2 °C) under the preferred steps. In addition, numerical methods can provide detailed information on temperature field along the DH pipeline. And the simulated temperature distribution along the pipeline at 9:00 and 9:30 Dec 15th, 2015 are shown in Fig. 10. As is shown that the temperature wave transports along the pipeline with time delay and temperature decay.

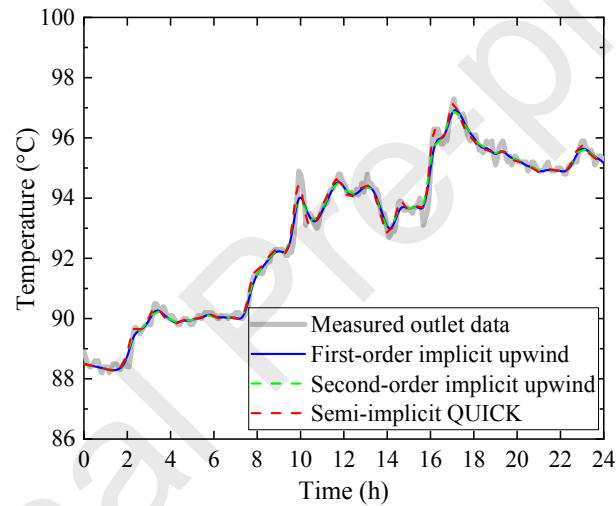


Fig.8. Temperature simulation under the preferred calculation steps

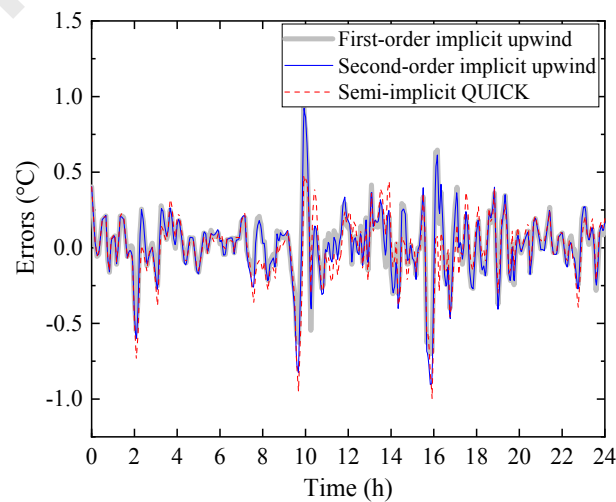


Fig.9. Calculation errors of the three methods with their preferred spatial and time steps

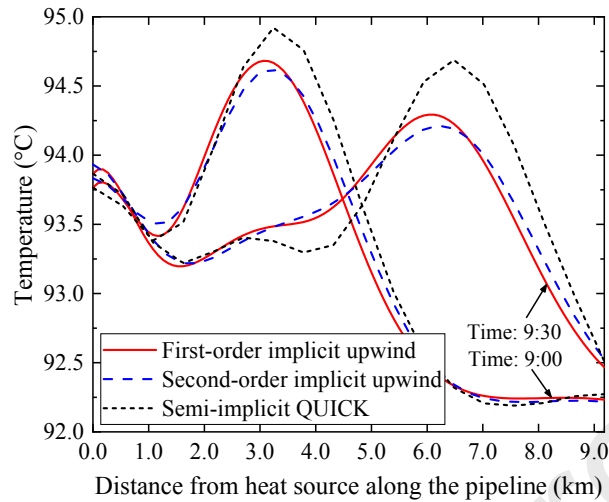


Fig.10. Temperature distribution along the pipeline at 9:00 and 9:30

Fluctuations of inlet temperature of DH pipeline can be well captured by the three methods with their preferred step sizes, but the computation burden and calculation errors are different for these methods. The second-order implicit upwind method performs best considering the least computation burden with satisfying simulation accuracy.

4.4. Simulation analysis with the second-order implicit upwind method

Thermal transients of DH pipeline are influenced by hot water mass flow rate within the pipeline, and this influence can be observed with the utilization of numerical method. The second-order implicit upwind method is applied to the thermal dynamic analysis of DH pipeline considering its good simulation performance. And the varying flow velocities are assumed, which are essentially the reflection of mass flow rate variations.

Fig. 11 shows the two flow velocity variation cases, $u_1(t)$ and $u_2(t)$. For $u_2(t)$, the flow velocity changes from 1.6 m/s to 2.0 m/s at 9:02. The inlet temperature variations of DH pipeline and simulated outlet temperature variations under $u_1(t)$ and $u_2(t)$ are shown in Fig. 12. It is indicated that the shape of outlet temperature propagation wave will be distorted due to the variation of flow velocity. Besides, Fig. 12 also shows that higher flow velocity will lead to faster temperature wave propagation and less heat loss, since the higher flow velocity will lead to the stronger thermal convection within the fluid and the more propagation time reduction of temperature wave, of which the heat loss can be decreased. And the time delay of temperature wave can be up to 76 minutes under $u_2(t)$, which is 20 minutes less than that under $u_1(t)$. The temperature decay at peak can be up to 1.0°C under $u_2(t)$ compared with the reduced peak value up to 1.1°C under $u_1(t)$. Fig. 13 shows the simulated temperature distributions along the pipeline under $u_1(t)$ and $u_2(t)$ at 9:00 and 9:30. Under $u_1(t)$, the two temperature distributions along the DH pipeline at 9:00 and 9:30 indicate the transportation of temperature wave. Besides, the temperature distributions under $u_1(t)$ and $u_2(t)$ at 9:30 also indicate that flow velocity increase will stretch the temperature wave along the DH pipeline.

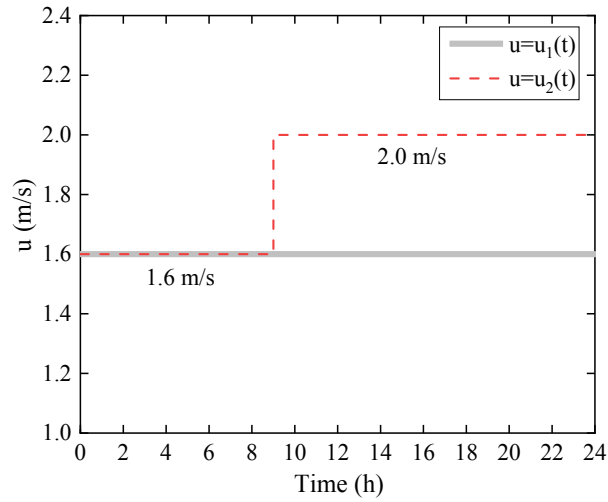


Fig.11. Two different flow velocity variations according to time

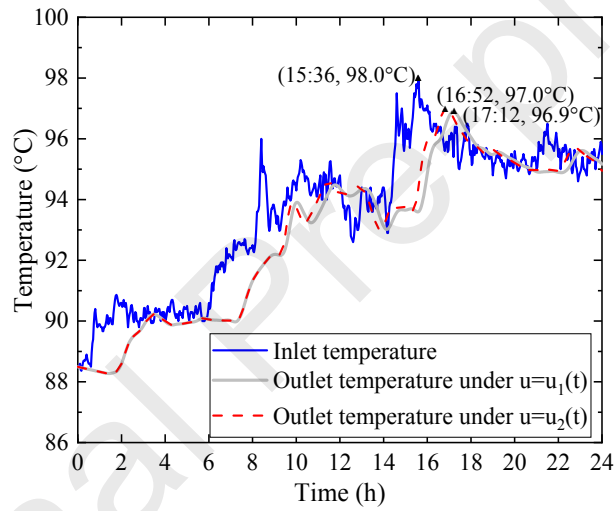


Fig.12. Simulation results of outlet pipeline temperature under different flow velocities

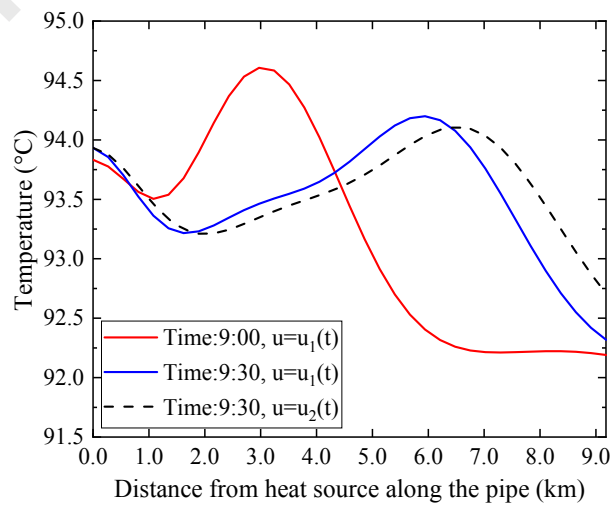


Fig.13. Temperature distribution along the pipeline under different flow velocities

5. Conclusions

In this paper, two novel iteration-free numerical methods, the second-order implicit upwind method and the semi-implicit QUICK method are developed for fast and accurate prediction of DH pipeline thermal dynamics. Validations of the two novel numerical methods are performed with measured data of a real DH pipeline. Comprehensive numerical experiments with different sizes of spatial and time steps are conducted to investigate the preferred spatial and time steps for fast and accurate simulation. And simulation analyses on thermal transients under varying flow velocities are performed with the application of the second-order implicit upwind method. The conclusions are as follows:

- (1) The influence of spatial step size on simulation accuracy of the three numerical methods are different for the case in this paper. As the size of spatial step increases, simulation errors monotonously increase for the first-order implicit upwind method, while maintaining consistent at the first stage and then increase as the spatial step size increases for the second-order implicit upwind method, and the transition point is $\Delta x/\Delta t = u^n$ in this case. Besides, the first stage embodies larger scales of spatial step with time step size increasing. For the semi-implicit QUICK method, simulation errors decrease at first and then increase, and the least simulation errors are obtained when the pipeline is divided into nine control volumes.

- (2) Appropriate calculation steps can be obtained by comparing the computation times of the three methods within acceptable simulation error. For the case studied in this paper, simulation errors are restricted to $\pm 1.0^{\circ}\text{C}$, and the spatial and time steps are recommended as $\Delta x = 90\text{ m}$ and $\Delta t = 60\text{ s}$ for the first-order implicit upwind method. As for the second-order implicit upwind method, the spatial and time steps are recommended as $\Delta x = 270\text{ m}$ and $\Delta t = 120\text{ s}$. For the semi-implicit QUICK method, the spatial and time steps are selected as $\Delta x = 540\text{ m}$ and $\Delta t = 60\text{ s}$.
- (3) With the preferred spatial and time steps, comparisons of the three different precision iteration-free numerical methods are conducted. Temperature fluctuations of outlet pipeline can be efficiently predicted by the three numerical methods without iteration. And the second-order implicit upwind method performs best considering the least computation burden, which is approximately four times faster than the other two methods.
- (4) The recommended second-order implicit upwind method is applied to the simulation analysis of DH pipeline under varying flow velocities. And higher flow velocity will lead to faster temperature wave propagation and less heat loss, as well as stretch the temperature wave along the DH pipeline.

Thermal dynamic prediction is essential to operation control of DH networks. The second-order implicit upwind method with the recommended spatial and time steps in this paper can efficiently predict thermal transient of DH pipeline. Based on this,

thermal dynamics of DH networks will be further simulated. And as the predictive control of DH networks has been widely discussed recently [15], the proposed second-order implicit upwind method can be utilized to predict thermal dynamics of DH networks and optimize the supply temperature of heat sources coupled with the optimization algorithm.

Acknowledgement

This work was supported by the Natural Science Foundation of Tianjin (No. 19JCQNJC07200) and the National Key R&D Program of China (No. 2018YFC0705000).

References

- [1] Lund H, Werner S, Wiltshire R, Svendsen S, Thorsen JE, Hvelplund F, et al. 4th Generation District Heating (4GDH). Integrating smart thermal grids into future sustainable energy systems. *Energy*. 2014; 68:1-11.
- [2] Wu CY, Gu W, Jiang P, Li ZY, Cai HY, Li BJ. Combined economic dispatch considering the time-delay of district heating network and multi-regional indoor temperature control. *IEEE Transactions on Sustainable Energy*. 2018; 9:118-127.
- [3] Gu W, Wang J, Lu S, Luo Z, Wu CY. Optimal operation for integrated energy system considering thermal inertia of district heating network and buildings. *Applied Energy*. 2017; 199:234-246.

- [4] Wang H, Meng H. Improved thermal transient modeling with new 3-order numerical solution for a district heating network with consideration of the pipe wall's thermal inertia. *Energy*. 2018; 160:171-183.
- [5] Wang JD, Zhou ZG, Zhao JN. A method for the steady-state thermal simulation of district heating systems and model parameters calibration. *Energy Conversion and Management*. 2016; 120:294-305.
- [6] Pan ZG, Guo QL, Sun HB. Interactions of district electricity and heating systems considering time-scale characteristics based on quasi-steady multi-energy flow. *Applied Energy* 2016; 167:230–243.
- [7] Hao L, Xu F, Chen Q, Wei MS, Chen L, Min Y. A thermal-electrical analogy transient model of district heating pipelines for integrated analysis of thermal and power systems. *Applied Thermal Engineering*. 2018; 139:213-221.
- [8] Li ZG, Wu WC, Shahidehpour M, Wang JH, Zhang BM. Combined heat and power dispatch considering pipeline energy storage of district heating network. *IEEE Transactions on Sustainable Energy*. 2016; 7:12-22.
- [9] Zheng JF, Zhou ZG, Zhao JN, Wang JD. Function method for dynamic temperature simulation of district heating network. *Applied Thermal Engineering*. 2017; 123:682-688.
- [10] Kunz VJ, Haldi PA, Sarlos G. Dynamic behaviour of district heating networks. *Fernwaerme Int*. 1991; 20:104-119.

- [11] Stevanovic VD, Zivkovic B, Prica S, Maslovaric B, Karamarkovic V, Trkulja V. Prediction of thermal transients in district heating systems. *Energy Conversion and Management*. 2009; 50:2167-2173.
- [12] Wang YR, You SJ, Zhang H, Zheng XJ, Zheng WD, Miao QW, et al. Thermal transient prediction of district heating pipeline: Optimal selection of the time and spatial steps for fast and accurate calculation. *Applied Energy*. 2017; 206:900-910.
- [13] Gabrielaitiene I, Bøhm B, Sunden B. Modelling temperature dynamics of a district heating system in Naestved, Denmark-A case study. *Energy Conversion and Management*. 2007; 48:78-86.
- [14] Gabrielaitienė I, Bøhm B, Sundén B. Dynamic temperature simulation in district heating systems in Denmark regarding pronounced transient behaviour. *Journal of Civil Engineering and Management*. 2011; 17:79-87.
- [15] Steer KCB, Wirth A, Halgamuge SK. Control period selection for improved operating performance in district heating networks. *Energy and Buildings*. 2011; 43:605-613.
- [16] Zhang T, Li ZG, Wu QH, Zhou XX. Decentralized state estimation of combined heat and power systems using the asynchronous alternating direction method of multipliers. *Applied Energy*. 2019; 248:600-613.
- [17] Sartor K, Dewalef P. Experimental validation of heat transport modelling in district heating networks. *Energy*. 2017; 137:961-968.

- [18] Van der Heijde B, Fuchs M, Tugores CR, Schweiger G, Sartor K, Basciotti D, et al. Dynamic equation-based thermo-hydraulic pipe model for district heating and cooling systems. *Energy Conversion and Management*. 2017; 151:158-169.
- [19] Biegler LT . Solution of dynamic optimization problems by successive quadratic programming and orthogonal collocation. *Computers & Chemical Engineering*. 1984; 8:243-247.
- [20] Tjoa IB , Biegler LT . Simultaneous solution and optimization strategies for parameter estimation of differential-algebraic equation systems. *Industrial & Engineering Chemistry Research*. 1991; 30:376-385.
- [21] Yancy-Caballero DM, Biegler LT, Guirardello R. Large-scale DAE-constrained optimization applied to a modified spouted bed reactor for ethylene production from methane. *Computers & Chemical Engineering*. 2018; 113:162-183.
- [22] Zhou SJ, Tian MC, Zhao YE, Guo M. Dynamic modeling of thermal conditions for hot-water district-heating networks. *Journal of Hydrodynamics*. 2014; 26:531-537.
- [23] Lim S, Park S, Chung H, Kim M, Baik YJ, Shin S. Dynamic modeling of building heat network system using Simulink. *Applied Thermal Engineering*. 2015; 84:375-389.
- [24] Dénarié A, Aprile M, Motta M. Heat transmission over long pipes: New model for fast and accurate district heating simulations. *Energy*. 2019; 166:267-276.

- [25] Chertkov M, Novitsky NN. Thermal transients in district heating systems. *Energy*. 2019; 184:22-33.
- [26] Wang H, Wang HY, Zhu T, Deng WL. A novel model for steam transportation considering drainage loss in pipeline networks. *Applied Energy*. 2017; 188:178-189.
- [27] Sartor K, Thomas D, Dewallef P. A comparative study for simulating heat transport in large district heating networks. *International Journal of Heat and Technology*. 2018; 36:301-308.
- [28] Guelpa E, Toro C, Sciacovelli A, Melli R, Sciubba E, Verda V. Optimal operation of large district heating networks through fast fluid-dynamic simulation. *Energy*. 2016; 102:586-595.
- [29] Guelpa E, Verda V. Compact physical model for simulation of thermal networks. *Energy*. 2019; 175:998-1008.
- [30] Guelpa E, Sciacovelli A, Verda V. Thermo-fluid dynamic model of large district heating networks for the analysis of primary energy savings. *Energy*. 2019; 184:34-44.
- [31] Schwarz MB, Mabrouk MT, Silva CS, Haurant P, Lacarrière B. Modified finite volumes method for the simulation of dynamic district heating networks. *Energy*. 2019; 182:954-964.

- [32] Duquette J, Rowe A, Wild P. Thermal performance of a steady state physical pipe model for simulating district heating grids with variable flow. *Applied Energy*. 2016; 178:383-393.
- [33] Versteeg H K, Malalasekera W. *An introduction to computational fluid dynamics*. 2th ed. England: Pearson Education Limited; 2007.
- [34] Tannehill JC, Anderson DA, Pletcher RH. *Computational fluid mechanics and heat transfer*. Bristol: Taylor & Francis; 1997.

Highlights

1. New numerical methods for thermal dynamic simulation of district heating pipeline
2. Validation of proposed numerical methods via one real district heating pipeline
3. Comparison of three different numerical methods on simulation performances
4. Preferred spatial and time steps for the three numerical methods
5. Thermal dynamic analysis of district heating pipeline under varying flow velocity